BIPM Capacity Building & Knowledge Transfer Programme

2025 BIPM - TÜBİTAK UME Project Placement

REPORT

Project Name	Study and Research on the Calibration of Spectroradiometers
Description	This project focused on acquiring practical and theoretical expertise in the calibration of spectroradiometers for photometric and radiometric applications. The work included hands-on training with reference spectral-irradiance sources and data-analysis methods to establish a traceable calibration procedure suitable for the Vietnam Metrology Institute (VMI).
Author, NMI	Nguyen Luong Hoang, Vietnam Metrology Institute (VMI), Vietnam
Mentor at TÜBİTAK UME	Doç.Dr. Çağrı Kaan Akkan, Optics Laboratory, TUBITAK National Metrology Institute (UME), Türkiye
Date	01/09/2025-26/09/2025

Motivation & Introduction

Reliable spectroradiometer calibration is essential for photometry, radiometry and the growing photovoltaic (PV) sector in Vietnam. At present, the Vietnam Metrology Institute (VMI) lacks the capability to perform such calibrations, creating a gap in the national quality infrastructure.

This placement at TÜBİTAK UME aimed to gain theoretical knowledge and hands-on experience in spectroradiometer calibration, study relevant international standards, and learn best practices from an advanced National Metrology Institute. The project objectives were to master calibration procedures, evaluate measurement uncertainty, and develop a foundation for establishing a spectroradiometer calibration service at VMI, thereby improving measurement traceability and supporting Vietnam's industry needs.

Research

1. CCD Array Spectrometer Fundamentals

Spectrometers can be classified by their light-collecting technique:

- **Scanning spectrometer** – Uses a single-channel detector (e.g., photomultiplier tube or silicon detector) and scans the spectrum by rotating a mirror. Because it collects light sequentially, it requires time to cover the whole spectrum and is less suited to measuring unsteady or rapidly varying light sources.
- **CCD array spectrometer** – Employs a multichannel charge-coupled device (CCD) to collect the entire spectrum simultaneously without mechanical movement. This makes it well suited to production inspection and transient light measurements. However, its spectral resolution depends on the CCD's specifications, and stray light caused by imperfect optical design can reduce measurement accuracy.

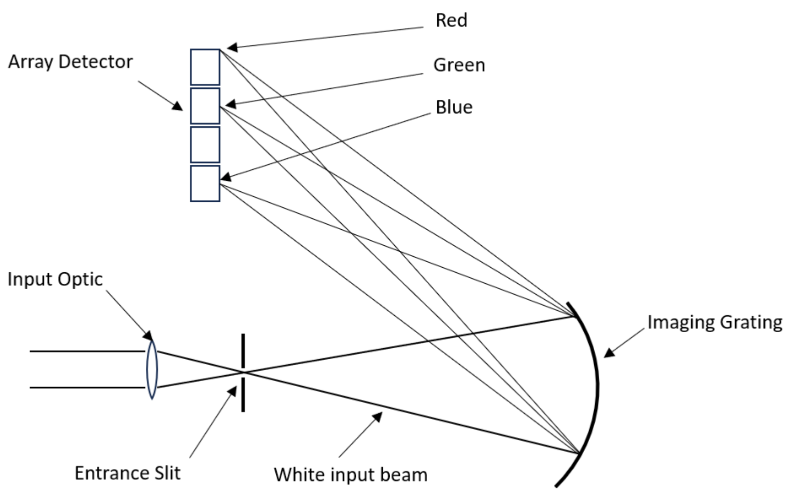

Fig . 1. Illustration of an array spectrometer composed of a fixed imaging grating and a fixed multipixel array detector.

2. Comparison of Denoising Methods

We compared two spectral denoising techniques: **Savitzky–Golay (SG)** filtering and **optimal cubic spline** smoothing.

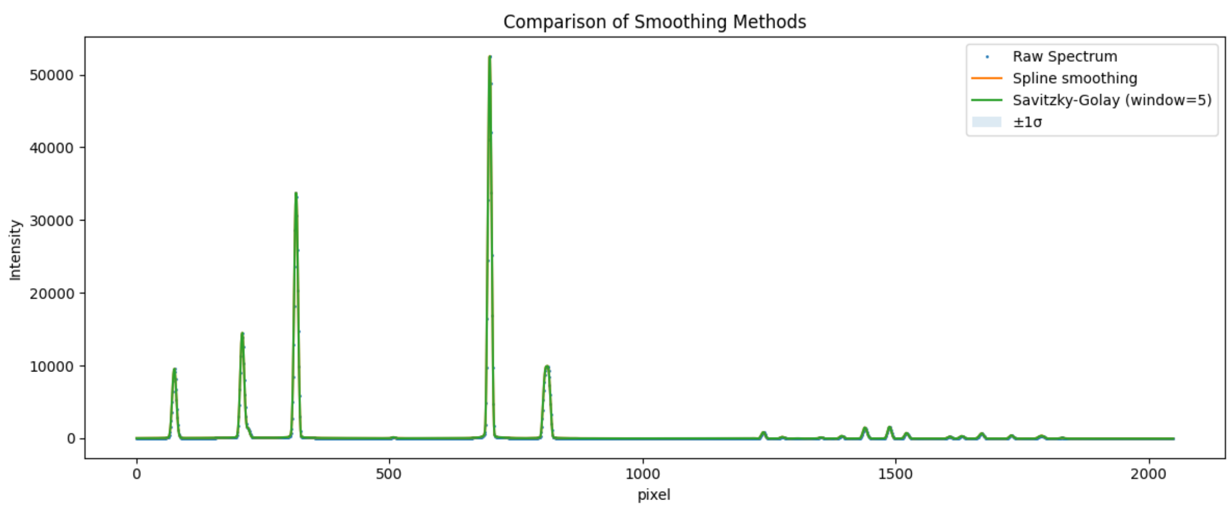

Fig. 1. Raw spectra from a Hg–Ar reference lamp were processed by both methods under the same mean-squared-error (MSE) constraint (cubic spline MSE = 68,93 count; Savitzky–Golay MSE = 67,45 count).

With Savitzky–Golay filtering, **peak positions were preserved**, whereas the cubic-spline method introduced slight pixel shifts at several low-intensity peaks—most notably near pixel 1439, 1522, 1631. (Figure 2).

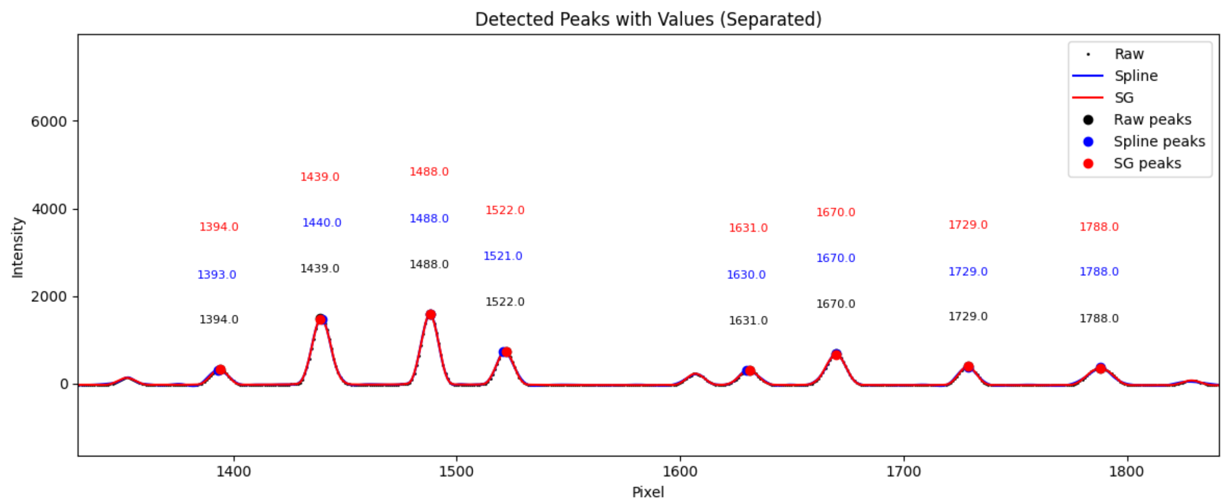

Fig. 2. Comparison of peak preservation after denoising: Savitzky–Golay (blue) vs. cubic spline (red) on Hg–Ar spectrum

Although the cubic-spline output appeared smoother overall, its residuals were larger in low-signal flat regions compared with the Savitzky–Golay result (Figure 3).

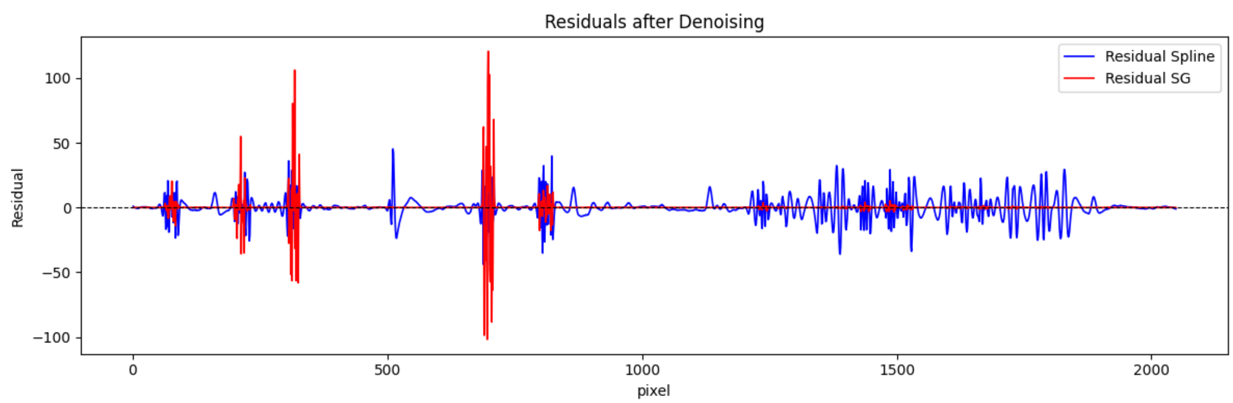

Fig. 3. Residual noise versus wavelength for Savitzky–Golay and cubic-spline smoothing.

Consequently, for Hg–Ar spectra that contain narrow emission lines used for wavelength calibration, denoising is not strictly necessary; if applied, Savitzky–Golay is recommended to maintain wavelength accuracy.
For smoother continua such as the FEL lamp spectrum used in spectral-irradiance calibration, the cubic-spline method can be advantageous for reducing high-frequency noise.

3. Wavelength Calibration

For individual emission lines requiring higher precision, peak centers were determined by nonlinear least-squares fitting to a Gaussian function,

$$Y = A.\exp\left(-\frac{(x-B)^2}{2.C^2}\right)$$

where A is the peak amplitude, B the centroid pixel, C the width. The Levenberg–Marquardt algorithm was used to obtain best-fit parameters and their standard uncertainties.

Representative Gaussian-fit results are summarized below:

pixel	pixel (Gaussian) [pixel]	Uncertainty [pixel]	N	RMS [count]
76	75,6377	0,0115	27	47,77
316	316,1914	0,0147	58	237,841
699	698,5412	0,0169	56	433,857
1239	1238,7288	0,0200	21	7,8259
1276	1276,3023	0,0102	18	0,990487
1352	1352,4048	0,0120	16	0,826211
1394	1393,7897	0,0117	18	1,85463
1439	1439,5062	0,0221	23	14,4089
1488	1488,0389	0,0184	22	13,3422
1522	1521,6858	0,0141	20	4,74417
1670	1669,7200	0,0314	23	9,13871
1788	1787,9831	0,0225	23	3,35799

During analysis, several spectral features were identified as blended or partially overlapping. For example, the emission near pixel 209 exhibited a subtle right shoulder, and the line near pixel 810 showed a broadened profile. To resolve these composite peaks, deconvolution with multiple Gaussians was applied (*Figures 4–5*).

Deconvolution results included, for example:

<table>
<tr><th>pixel (Gaussian) [pixel]</th><th>Uncertainty [pixel]</th><th>N</th><th>RMS [count]</th></tr>
<tr><td>209,796</td><td>0,0136</td><td rowspan="2">45</td><td rowspan="2">71,0339</td></tr>
<tr><td>221,632</td><td>0,1617</td></tr>
<tr><td>807,731</td><td>0,1713</td><td rowspan="2">30</td><td rowspan="2">76,3068</td></tr>
<tr><td>815,150</td><td>0,0794</td></tr>
</table>

It is noteworthy that while deconvolution successfully separated overlapping lines, the associated standard uncertainties were significantly larger than those for isolated peaks. Therefore, unless such blended lines are of particular metrological relevance, they are typically excluded from the final calibration dataset.

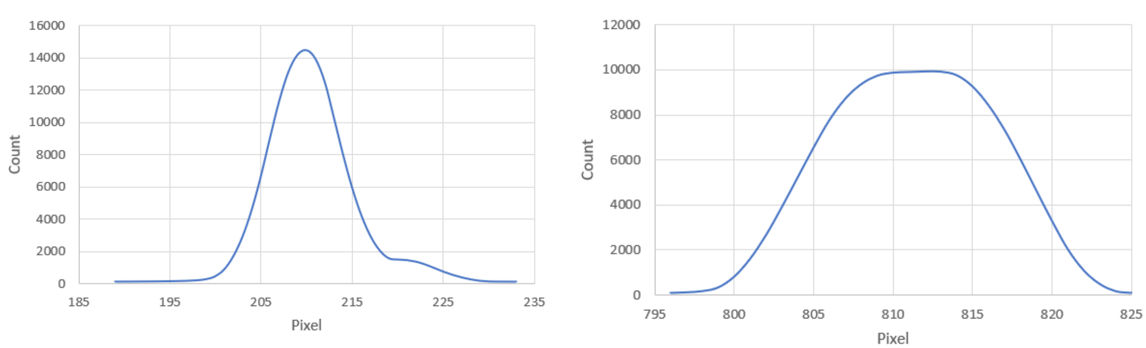

Fig. 4. Raw spectrum with convolution

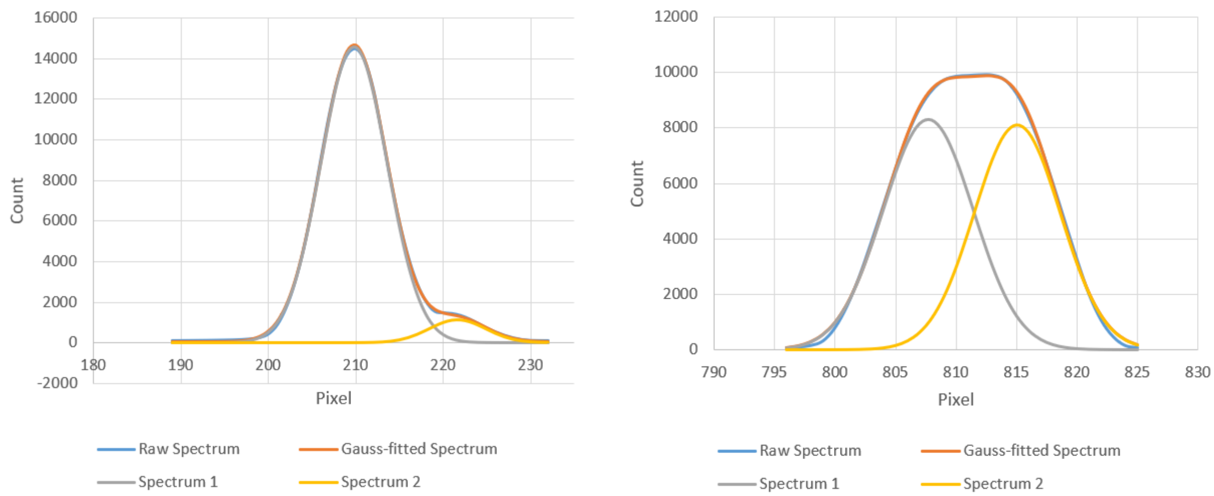

Fig. 5. Deconvolved spectrum

To establish the wavelength accuracy of the CCD spectroradiometer, a mercury–argon line-spectrum lamp was employed as the primary reference. The pixel-to-wavelength relationship was modeled by a third-order polynomial:

$$\lambda = a_0 + a_1 p + a_2 p^2 + a_3 p^3$$

where ppp is the pixel number and a_0,a_1,a_2,a_3 are the coefficients determined by ordinary least squares (OLS).

The combined standard uncertainty in wavelength arises predominantly from the uncertainties of these coefficients, yielding a calibration uncertainty of approximately 0,11 nm.

Representative results are given below:

pixel	Standard Wavelength [nm]	Polynomial Fit Wavelength [nm]	Error [nm]	Polynomial Fit [nm]
75,638	365,010	364,98	-0,03	0,106
316,191	435,840	435,88	0,04	0,076
698,541	546,080	546,11	0,03	0,087
1238,729	696,540	696,42	-0,12	0,048
1276,302	706,720	706,63	-0,09	0,047
1352,405	727,290	727,21	-0,08	0,044
1393,790	738,400	738,35	-0,05	0,043
1439,506	750,390	750,60	0,21	0,042
1488,039	763,510	763,55	0,04	0,041
1521,686	772,400	772,50	0,10	0,041
1669,720	811,530	811,55	0,02	0,057
1787,983	842,460	842,37	-0,09	0,093

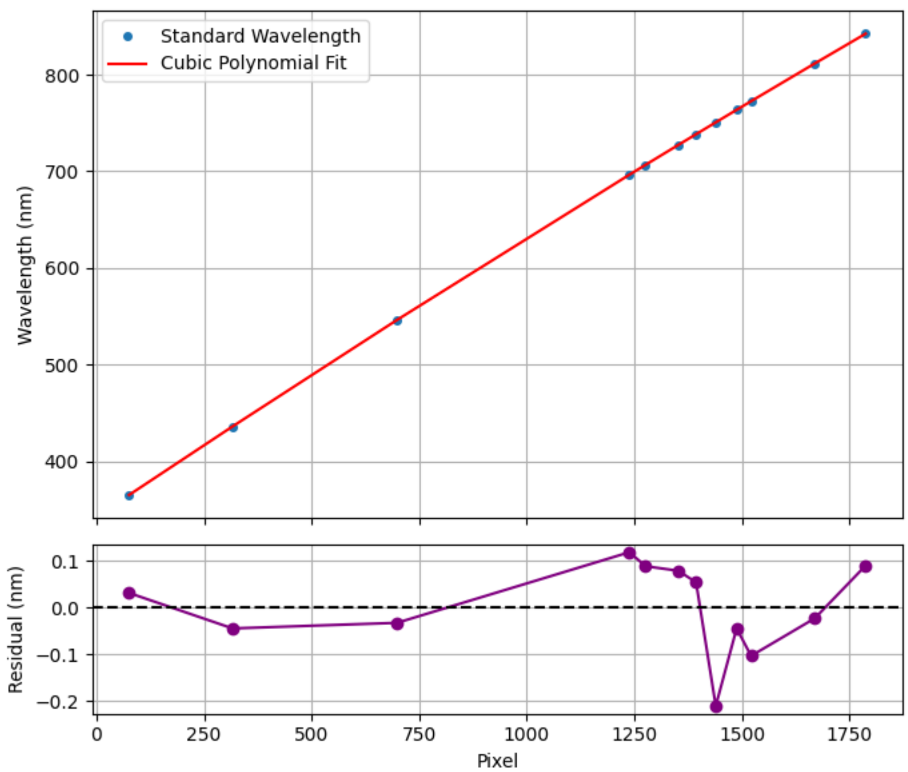

Fig. 6. Cubic polynomial wavelength calibration of the Hg–Ar spectrum and corresponding residuals.

Combined and Expanded Measurement Uncertainty

Uncertainties were propagated according to the GUM law of propagation of uncertainty, using sensitivity coefficients derived from the polynomial model.
Example at 365 nm:

Component	Value	Distribution	u(component)	Sensitivity coeff
Lamp certificate (λ)	365,01	normal	0,01 nm	1
Gaussian fit	-	normal	0,0115 pixel ≈ 0,0034 nm	1
Polynomial fit	-	normal	0,106 nm	1
Combined uc	-	-	0,107 nm	

Similar calculations were performed for all calibration lines:

Standard Wavelength [nm]	Fit Wavelength [nm]	Error [nm]	Combined u_c [nm]
365,010	364,98	-0,03	0,107
435,840	435,88	0,04	0,077
546,080	546,11	0,03	0,088
696,540	696,42	-0,12	0,049
706,720	706,63	-0,09	0,048
727,290	727,21	-0,08	0,045
738,400	738,35	-0,05	0,044

750,390	750,60	0,21	0,044
763,510	763,55	0,04	0,042
772,400	772,50	0,10	0,042
811,530	811,55	0,02	0,058
842,460	842,37	-0,09	0,094

The expanded measurement uncertainty $U=k\cdot u_c$ was obtained with coverage factor k=2.

4. Spectral Irradiance Calibration

Two principal approaches exist for spectral irradiance calibration: the **source-based method** and the **detector-based method**. In this work, we adopted the detector-based approach to calibrate the spectroradiometer. The calibration setup consisted of an FEL-type quartz halogen lamp as the reference source, a three-element silicon trap detector, precision band-pass interference filters, and a well-characterized aperture. These components allowed the determination of the lamp's spectral irradiance at selected wavelengths, providing traceability to primary standards.

The photocurrent i of the filter radiometer, with known spectral responsivity R(λ), when exposed to the spectral irradiance E(λ) of the lamp and filtered by an interference filter of transmittance τ(λ), is expressed as

$$i = A \int_{\lambda} E(\lambda) R(\lambda) \tau(\lambda) d\lambda$$

where A is the aperture area of the filter radiometer.

The spectral irradiance of the source at the filter effective wavelength, λ_{eff}, is given by

$$E(\lambda_{eff}) = \frac{i}{A \int_{\lambda} R(\lambda)\tau(\lambda) d\lambda}$$

The effective wavelength of the filter is defined as

$$\lambda_{eff} = \frac{\int_{\lambda_1}^{\lambda_2} \lambda \tau(\lambda) d\lambda}{\int \tau(\lambda) d\lambda}$$

FEL-type lamps are advantageous because they produce a continuous spectrum free of absorption or emission lines, and their spectral distribution closely resembles that of a Planck radiator. Accordingly, the spectral irradiance values determined at discrete filter wavelengths can be interpolated using an analytical approximation of the lamp's spectral distribution:

$$E_c(\lambda) = (1 + A_1 \lambda) e^{(A_0 + \frac{A_2}{\lambda})} \lambda^{-5}$$

Here A_0, A_1 and A_2 are fitting parameters. The exponential term is an approximation to the theoretical spectral radiance of a blackbody. This function includes the effect of the spectral emissivity of the tungsten and the spectral transmission of the lamp bulb.

The spectra measured by the spectroradiometer were further processed using **optimal cubic-spline smoothing** to suppress high-frequency noise. Since accurate spectral irradiance determination requires linearity in detector response, a **CCD linearity correction** was also applied. This was achieved by recording lamp spectra at approximately 13 different exposure times. The measured response was fitted with an eighth-order polynomial (without constant term, since the CCD output is zero in the absence of light) [2], thereby providing a correction function valid across the detector's dynamic range.

Stray-light correction was implemented following the method of Zong et al. [1], which characterizes the instrument's response to monochromatic radiation at a discrete set of wavelengths. This method does not require fine-tuning of the monochromator and can be implemented with fixed-wavelength spectral line sources, making it practical for calibration laboratories.

Finally, the **spectral responsivity** of the spectroradiometer was obtained as the ratio between the calibrated spectral irradiance of the FEL lamp and the corresponding DUT measurement:

$$S(\lambda) = \frac{E_c(\lambda)}{E_{dut}(\lambda)}$$

This responsivity function (expressed in counts per W.m^{-2}.nm^{-1}) establishes the traceable calibration of the instrument, enabling accurate conversion of raw CCD counts into absolute spectral irradiance values.

Uncertainty budget

Component	Value / Method	Distribution	Sensitivity coeff
Trap detector responsivity R(λ)	Type B, certificate	Normal	1
Filter transmittance τ(λ)	Type B, certificate	Normal	1
Aperture area A	Type B, certificate	Normal	1
Photocurrent i	Type B, certificate	Normal	1
Lamp stability	Type A, Type B	Normal	1
Alignment / distance error	-	Normal	1
Spectral modeling $E_c(\lambda)$	Least-squares fit residuals	Normal	1
Denoising (signal processing)	cubic-spline smoothing	Normal	1
CCD linearity correction	Least-squares fit residuals	Normal	1
Stray-light correction	LSF repeatability + matrix inversion, per Zong et al. 2006	Normal	1
Repeatability	Type A	Normal	1

Conclusions and Future Work

The training course met its objectives by providing me with the knowledge and hands-on practice needed for spectroradiometer calibration. I learned how to perform wavelength and irradiance calibration, apply data processing techniques such as Gaussian fitting, polynomial calibration, and denoising, and carry out essential corrections including stray-light and detector linearity adjustments.

Now, I am prepared to develop a formal calibration procedure for spectroradiometers at the Vietnam Metrology Institute (VMI). Future work will focus on drafting this procedure, refining the evaluation of measurement uncertainty, and preparing for interlaboratory comparisons to strengthen VMI's capabilities in optical metrology.

Acknowledgements

I would like to express my sincere gratitude to Assoc. Prof. Dr. Cagri Kaan Akkan, my main supervisor, and Assoc. Prof. Dr. Ferhat Sametoglu for their dedicated guidance, generous knowledge sharing, and for teaching me the methodology of spectroradiometer calibration.
My thanks also extend to TÜBİTAK UME for kindly hosting this training, and to the Physikalisch-Technische Bundesanstalt (PTB) for their collaboration and support through the BIPM Capacity Building & Knowledge Transfer Programme. Their assistance and encouragement have been invaluable to the success of this training and to my professional development in optical metrology.

References

[1] Y. Zong, S. W. Brown, B. C. Johnson, K. R. Lykke, and Y. Ohno, "Simple spectral stray light correction method for array spectroradiometers," Appl. Opt., vol. 45, no. 6, pp. 1111–1119, Feb. 2006.
[2] Han-Kuei Fu, Yen-Liang Liu, Tzung-Te Chen, Chien-Ping Wang, and Pei-Ting Chou, "The Study of Spectral Correction Algorithm of Charge-Coupled Device Array Spectrometer," IEEE TRANSACTIONS ON ELECTRON DEVICES, VOL. 61, NO. 11, NOVEMBER 2014
[3] J. Zhou, X. Chen, Y. Ji, Y. Chen, and W. Shen, "Spectral calibration for convex grating imaging spectrometer," Proc. SPIE 9045, 90451U (2013).